Optimally Curved Arc Source for Sound Reinforcement

Lukas Gölles[1], Franz Zotter[2]

[1] Graz, University of Technology & University Of Music And Perfoming Arts Graz, Email: goelles.lukas@gmail.com

[2] Institute Of Electronic Music and Acoustics, University Of Music And Perfoming Arts Graz, Email: zotter@iem.at

Introduction

Today, high-quality supply of large audience areas with consistently reinforced sound pressure levels typically considers line-source loudspeaker arrays. For instance, Toole [1] describes the application of line sources as well as the idea of constant direct-sound level for all listener positions. Waveguides were essential technical achievements in line-source arrays, e.g., C. Heil's Diffuseur d'Onde Cylindrique (DOSC, 1992) [2] and E. Vincenot's and F.Deffarge's Hyperbolic Reflective Wavesource (HRW, 2003) [3]. Both inventions enable line-source arrays with good directivity behaviour at mid and high-frequencies, i.e., minimal grating lobes, minimal comb filtering or phasing of neighbouring loudspeaker cabinets in the stack. Wavefront Sculpture Technology by Urban et al. [4] relates to the waveguide technology and lays the basis for state-of-the-art design of sound-pressure coverage by curved sources built from arrays, see also [5]. Smith [6], Straube et al. [7, 8] further discuss the modelling and optimization of the shape of such line-source loudspeaker arrays. The discussion of such line-source arrays in combination with the Fourier-transform and 2.5D WFS theories is carried on in the PhD thesis of Schultz [9].

Most of these works deal with discrete line source elements and their fitting process to supply the audience area, yielding suitable splay angles between discrete line-source elements. Literature appears to lack a continuous theory relating the contour of an arc source with the resulting sound pressure level. Our paper intends to present and discuss a suitable theory using the stationary phase approximation to calculate the sound pressure level in response to an integral of a Green's function over a variable contour whose optimal shape is yet to be found, which gets rewarded by yielding a second-order nonlinear differential equation defining the family of contours that we term Optimally Curved Arc Source (OCAS).

Optimally Curved Arc Source theory

For an arc-shaped source to evenly cover a specific audience area, we evaluate the sound pressure by the contour integral of a Green's function $G(R) = \frac{e^{-ikR}}{4\pi R}$ over the source positions $\boldsymbol{x}(s) = \begin{bmatrix} x & v \end{bmatrix}^T$ with the horizontal and vertical coordinates x, v depending on the length parameter s along an unknown contour C,

$$p = \int_C G(R)\,\mathrm{d}s = \int_C \frac{e^{-ikR}}{4\pi R}\,\mathrm{d}s\,. \tag{1}$$

The result is received at $\boldsymbol{x}_r = \begin{bmatrix} x_r & 0 \end{bmatrix}^T$ located in the horizontal plane below the source contour, defining the distance $R = \sqrt{(x - x_\mathrm{r})^2 + v^2}$. The integral in s is now rewritten in terms of the horizontal contour coordinate x, which is accomplished using the rectangular triangle between $\mathrm{d}x$ and $\mathrm{d}v$ yielding the natural length $\mathrm{d}s^2 = \mathrm{d}x^2 + \mathrm{d}v^2$, and hence for $\mathrm{d}s = \mathrm{d}x\sqrt{1 + v'^2}$, with $v' = \frac{\mathrm{d}v}{\mathrm{d}x}$, as shown in Fig. 1. The stationary phase approximation for an integral over a phasor that oscillates rapidly along the integration path permits to relate the result of the integral to a stationary-phase point $\boldsymbol{x}_s$, which is a point assigned to the point of observation $\boldsymbol{x}_r$. In the given scenario, the phase gets stationary at the point $\boldsymbol{x}_s$ with maximal phase, i.e. minimal distance R where $R' = 0$,

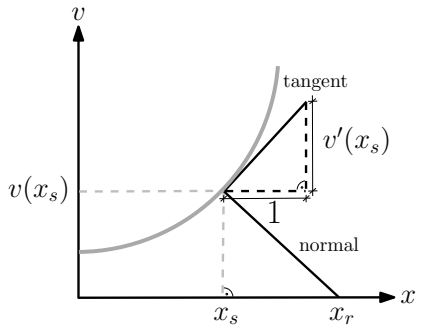

Figure 1: Geometry of tangent and normal at stationary point and its corresponding reference point for a curved source.

$$p = \int \frac{e^{-ikR}}{4\pi R}\sqrt{1 + v'^2}\,\mathrm{d}x \approx \frac{e^{-ikR}}{4\pi R}\sqrt{\frac{2\pi}{kR''}}\sqrt{1 + v'^2}\,e^{-i\frac{\pi}{4}}\Bigg|_{\boldsymbol{x}_s}$$
$$\approx \frac{e^{-i\left(kR + \frac{\pi}{4}\right)}}{\sqrt{8\pi k}}\sqrt{\frac{1 + v'^2}{RR''}}\Bigg|_{\boldsymbol{x}_s}. \tag{2}$$

This stationary-phase point is related to the point of observation by $\frac{x_r - x_s}{v} = v'$ as shown graphically in Fig. 1, i.e. $R = v\sqrt{1 + v'^2}$. Disregarding common factors and the frequency dependency $\frac{1}{\sqrt{k}}$, we desire for the pressure magnitude to become independent of the listening position for an Optimally Curved Arc Source (OCAS). To this end, the square-root above needs to be constant, $c = \frac{RR''}{1 + v'^2}$. Employing the derivatives defining R'' and the stationary-phase R, any ideal contour therefore needs to solve a second-order nonlinear differential equation,

$$c = v\sqrt{1 + v'^2} + \frac{v^2 v''}{\sqrt{1 + v'^2}}\,. \tag{3}$$

Solution

As there is no well-defined mathematical function solving the differential equation (3), the solution is rather calculated by numerical methods. The Euler Method allows to

solve the problem with sufficient precision as long as the step size stays accurately small. To make this method usable for the second-order differential equation, a set of first-order differential equations is necessary. Setting $v = \eta$, $v' = \zeta' = \eta$ and $v'' = \eta' = f(c, \zeta, \eta)$ yields a first-order system,

$$\begin{bmatrix} \zeta' \\ \eta' \end{bmatrix} = \begin{bmatrix} \eta \\ c\,\frac{\sqrt{1+(\eta')^2}}{\zeta^2} - \frac{1}{\zeta} - \frac{\eta^2}{\zeta} \end{bmatrix} = \begin{bmatrix} \eta \\ f(c, \zeta, \eta) \end{bmatrix}. \quad (4)$$

For each row, the Euler Method has to be applied so that the system can be solved numerically by

$$\zeta_{n+1} = \zeta_n + \Delta x\, \eta_n \quad (5)$$
$$\eta_{n+1} = \eta_n + \Delta x\, f(c, \zeta_n, \eta_n)\,. \quad (6)$$

This solutions allows to build up a simple webbased solver using JavaScript[1].

For solving the differential equation numerically, the initial conditions for v and v' are needed. Typically one would calculate the source for any positions starting at $x = 0$. For example, the initial conditions $v(0) = 1$ and $v'(0) = 0$ as initial height and slope are used in Fig. 2 with either $c = 10$ or $c = 15$. As shown in Fig. 3, a higher value for c yields a higher initial curvature and peak curvature. For $v(0) = 1$, $v'(0) = 0$, the parameter at $x = 0$ should not be lower as $c > 1$ to yield an upward curve, as $c = 1 + v''(0)$.

By inspecting Fig. 3 in detail, the curvature apparently gets negative, which cannot be realized by all-positive line-source array splay angles, or under the reasonable constraint to convex curvature. The transition at $v'' = 0$ is marked by a dotted line, and we would like to find this intersection. Eq. (3) describes the relation between v, v' and c, and we insert $v'' = 0$ to get the condition at which positive curvature ends

$$c = v\,\sqrt{1 + v'^2} = R\,. \quad (7)$$

The farthest reachable distance of observation to the upper end of the contour is therefore limited by $R \leq c$.

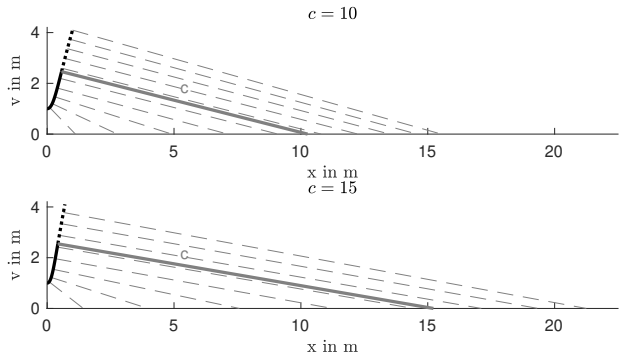

Figure 2: Numerical solutions of the differential equation ($c = 10$ and $c = 15$, initial conditions $v = 1$ and $v' = 0$) with normals connecting the contour with points of observations, dotted lines denote points with $v'' < 0$.

[1] https://lukas_goelles.iem.sh/ocas_web/

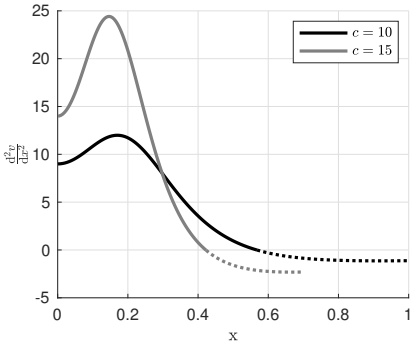

Figure 3: Curvature of the resulting contours shown in Fig. 2, dotted lines denote $v'' < 0$.

Simulations in big systems

A classical large-scale line-source array sound reinforcement scenario is assumed where two line-source arrays are placed left and right of a stage. The size of the audience area is 30 m × 30 m and the simulation height for the audience is 1.6 m (standing audience). For each side there is a maximum of six line-source elements, L'Acoustics[2] KARA II, available. The differential equation is solved by using the following settings: $c = 54$, $v(0) = 2$ and $v'(0) = 1.04$. By using the height of one cabinet 25.2 cm the solution is discretized and in the simulation software Soundvision[3] the points of observation were entered as accurately as possible. The finite number of available splay angles between the line-source array elements only permits to approximate the ideal points of observation. Table 1 shows the comparison between the theoretical and practical points of observation for each element. Fig. 4 shows the resulting level map of the simulation done in Soundvision.

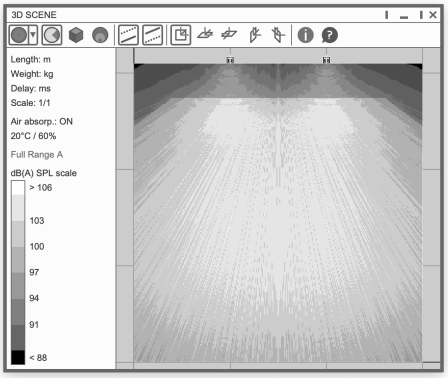

Figure 4: Resulting coverage for an OCAS shape like line-source array in a stereo setup, simulated by Soundvision with six KARA II (Grid: 10 m × 10 m)

To host a large audience for 3D sound reinforcement, the new OCAS is helpful to maintain the directional balance until the outmost listening positions in the audience. To evaluate the mean absolute localisation error over the same listening area as before, the extended $\boldsymbol{r}_E$ vector model is used [10]. Encoding is done by spherical har-

[2] https://www.l-acoustics.com/products/kara-ii/

[3] https://www.l-acoustics.com/products/soundvision/

Enclosure Nr.	Theoretical	Practical usable
1	5.29	5.29
2	11.46	10.58
3	17	17.4
4	22.03	21.44
5	26.64	27.57
6	30.62	29.87

Table 1: Points of observation of the resulting curved line-source.

monics as described in [11]. The AllRAD (all-round Ambisonic decoding) decoder is used to calculate the sound field for the loudspeaker arrangement [12]. As [13] describes the negative effect of delay compensated systems on the sweet area, only amplitude compensation to a central listening position is done.

Fig. 5 shows the mean average localization error for an arrangement of OCAS sources for a fifth order Ambisonic playback scenario along the horizon compared to a setup with conventional loudspeakers, modelled as point sources. An approach considering the plausible sweet area is mentioned in [14]: The audience area is therefore defined as $\frac{2}{3}$ of the radius of the setup. At a radius of 10 m in the plot of the point source arrangement, which corresponds to $\frac{2}{3}$ of the setup radius, the 10° mark is reached. Searching this mark in the OCAS simulation results will yield a radius of 14.5 m. This mark has to be reduced to 13 m as the initial condition of the differential equation v' was set to 2. In this way only very close to the sources the mean absolute localization error is noticeable high. For the OCAS a rectangular sweet area of 26 m × 26 m (676 m^2) may be found for which the error stays below 10° and for the point source arrangement, this rectangle is defined by 20 m × 20 m (400 m^2), which yields a factor of 1.69 in between the resulting areas. The expected benefits are assumed to be most noticeable at listening positions at the outer rims of the seating area.

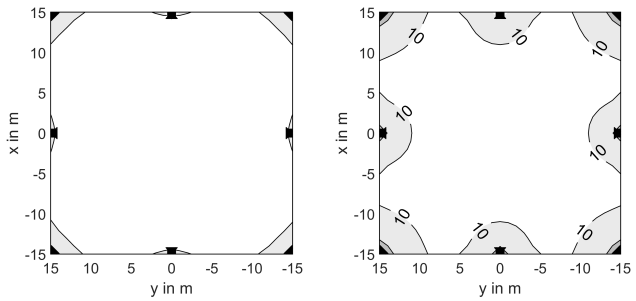

Figure 5: Mean average localisation error for panning along the horizon for an arrangement with OCAS (left) compared to an arrangement with point sources (right).

Compact Waveguide solution

For a more compact OCAS design, DOSC and HRW waveguides typically target a vertically flat or circular output which makes them only useable for large implementation of the OCAS. We envision a waveguide that allows to vertically shape the wavefront perfectly in the OCAS shape, therefore the isophasic waveguide should

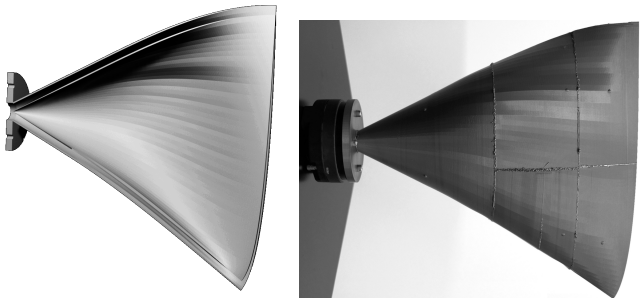

Figure 6: Parallel shells between which the waves are directed with flange for the compression driver cut along the y-axis to view inside the waveguide (left) and resulting 3D printed waveguide with mounted driver. (right)

precisely assume the particular custom curve resulting as a solution.

The room for which the compact waveguide should work is the IEM CUBE, a 10.3 m × 12 m × 4.8 m studio with reverberation time of 0.5 ms. Employed as high frequency transducer of a horizontal loudspeaker, the OCAS should be able to cover a distance of approximately 9 m. The first seat row is placed at $x_R = 0.5$ m which yields the initial condition for the first derivative $v' = 1$ by choosing $v = 0.5$ and the curvature/distance parameter is set to $c = 15$.

The prototype is designed for frequencies above 1kHz, fed by a single compression driver (SB Audience BIANCO-44CD-T), and built as a 3D-printed waveguide. 3D polynomials are calculated so that the length of each path starting from the driver and ending at the waveguide orifice is equal. The polynomials end perpendicular to the tangent at the orifice to fulfill the property of a stationary-phase point. The resulting polynomials shape the interior body of the waveguide and a distance of 127 mm is used to build the external shell. Fig. 6 shows the resulting prototype.

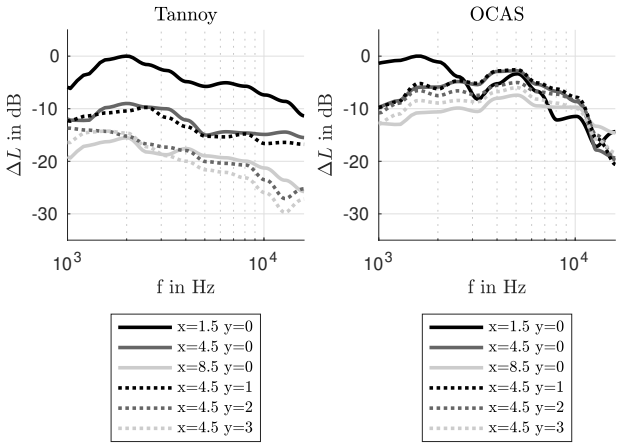

Figure 7: Third-octave averaged direct sound frequency response for different positions (sources are located at $x = 0$ and $y = 0$).

Fig. 7 shows the measured third-octave averaged direct-sound frequency response for different receiver positions

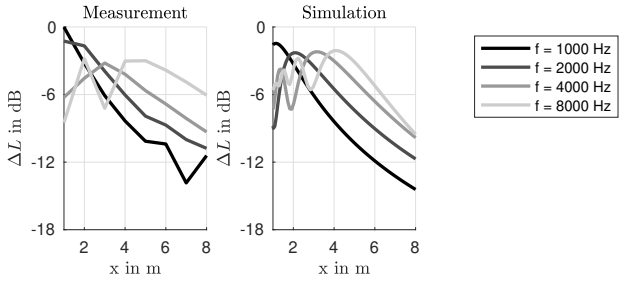

Figure 8: Measured vs. calculated direct-sound level.

of the OCAS compared to a point-source like loudspeaker, Tannoy Systems 800. The primary feature concerns the position dependent level differences that are not as distinctively pronounced for the OCAS as they are for the Tannoy loudspeaker. For the OCAS, the measured amplitude decrease at high frequencies corresponds to $-3\,\mathrm{dB/oct}$ plus the transducer response and uniformly effects every receiver position. In the rather uniform responses of the OCAS, only position 1, which is very close to the source, sticks out. Fig. 8 shows the comparison between the simulated direct-sound level and the measured one. Compared to the simulated results, the graphs of the OCAS prototype follow nearly identical trends. For 8000 Hz the simulated roll-off is not as steep in the measured results. This result most distinctively confirms the applicability of the OCAS theory and waveguide design presented here.

Conclusion and Outlook

We were able to present a novel source type in sound reinforcement that targets a constant direct-sound level (as an exemplary target). We call the resulting source that produces wave fronts emerging form an arc-shaped, linear contour Optimally Curved Arc Source (OCAS). We could prove that the OCAS produces consistent and applicable results when discretized to fit line-source cabinets of a line-source array simulated in Soundvision, making it work with existing line array technology. Exceeding the stereo setup, OCAS was shown to be capable of improving immersive 3D or surround reproduction in comparison to point-source loudspeakers, by enlarging the sweet area together with the improvements in even sound pressure coverage. Finally, OCAS was used as curvature design of an equi-phase linear waveguide orifice, for which a compact prototype was built to serve medium-scale sound reinforcement applications. Measurements with the waveguide could confirm the expected improvements in direct-sound coverage.

Further work should consider modifying and psychoacoustically optimizing the direct-sound target. Moreover, new strategies for designing cost-efficient wide-band OCAS systems could be rewarding to improve medium-sized immersive sound reinforcement for 50-250 listeners. We filed a provisional patent application.

References

[1] F. Toole, *Sound Reproduction: The Acoustics and Psychoacoustics of Loudspeakers and Rooms* . Elsevier Ltd, 2008.

[2] C. Heil, "Sound wave guide," U.S. Patent 5163167A, Oct. 1992.

[3] E. Vincenot and F. Deffarges, "Sound-Producing Device With Acoustic Waveguide," U.S. Patent 6585077B2, Jul. 2003.

[4] M. Urban, C. Heil, and P. Bauman, "Wavefront sculpture technology," *J. Audio Eng. Soc.*, vol. 51, 2003.

[5] M. S. Ureda, "Analysis of loudspeaker line arrays," *J. Audio Eng. Soc.*, vol. 52, no. 5, 2004.

[6] D. L. Smith, "Discrete-Element Line Arrays-Their Modeling and Optimization," *J. Audio Eng. Soc.*, vol. 45, no. 11, 1997.

[7] F. Straube, F. Schultz, M. Makarski, S. Spors, and S. Weinzierl, "Evaluation Strategies for the Optimization of Line Source Arrays," in *59th AES Conf.*, Jul., 2015.

[8] F. Straube, D. Albanés, F. Schultz, and S. Weinzierl, "Zur Optimierung der Krümmung von Line Source Arrays," *DAGA*, Mar., 2017.

[9] F. Schultz, "Sound Field Synthesis for Line SourceArray Applications in Large-ScaleSound Reinforcement," Ph.D. dissertation, 2016.

[10] E. Kurz and M. Frank, "Prediction of the listening area based on the energy vector," in *Proc. ICSA*, Sept., 2017.

[11] F. Zotter and M. Frank, *Ambisonics: A Practical 3D Audio Theory for Recording, Studio Production, Sound Reinforcement, and Virtual Reality*, 2019.

[12] F. Zotter, H. Pomberger, and M. Noisternig, "Energy-Preserving Ambisonic Decoding," *Acta Acustica united with Acustica*, vol. 98, 2012.

[13] M. Frank, "How to make Ambisonics sound good," in *Proceedings of Forum Acusticum*, Sept., 2014.

[14] M. Frank and F. Zotter, "Exploring the perceptual sweet area in Ambisonics," in *Proc. AES 142nd Conv.*, May, 2017.